MATERIALS AND METHODS

Mouse alleles and transgenic lines. The *Nkx2.5cre* transgenic line has been previously described (*S1*). This line uses a 5.4kb region of homology whereby Cre recombinase is fused to exon 2 of *Nkx2.5* to direct Cre expression in cardiac-specific cells. *Nkx2.5cre* mice were mated to mice carrying a floxed allele of *ww45/Salvador, lats2/Warts, or mst1-2/Hippo* and extracted DNA from yolk sacs or tails of resultant progeny was genotyped. Genotyping primers are as follows: *Nkx2.5cre* 5'-TTGTCCAAGCCACTTAGGCA-3', 5'-ATTCAACTTGCACCATGCCGC-3'; $Salv^{flox/flox}$ 5'-TGTCAGTGTAAAATGGCCACA-3', 5'-TTGGGAATGGTTTTACAAGTT T-3'; $Lats2^{flox/flox}$ 5'- GCGCATGCCTTTAATCCTAGC-3', 5'- GCACACATTCCCCTCCACTGAC-3', $Mst1^{flox/flox}$ 5'-CCTGCTTCAGTGTTGGCTCTT-3', 5'-TAGACCAGCCAGGGCTAGAGT-3', $Mst2^{flox/flox}$ 5'-GTTCAGGGTCCCACCAAGAGT-3', 5'-TGTCTAGCTGCTGATGACACT-3'. Control: $Nkx2.5^{Cre/+}$; $Salv^{flox/+}$ for Figures 1-4, S1, S3, and S5. *Salv CKO*: $Nkx2.5^{Cre/+}$; $Salv^{flox/flox}$ for all figures. Control: $Nkx2.5^{Cre/+}$; $Mst1^{flox/+}$; $Mst2^{flox/+}$ for figures S2A and S4D. control: $Nkx2.5^{Cre/+}$; $lats2^{flox/+}$ for figures S2B and S4D. *Lats2 CKO*: $Nkx2.5^{Cre/+}$; $Lats2^{flox/flox}$ for all figures. *Mst1-2 CKO*: $Nkx2.5^{Cre/+}$; $Mst1^{flox/flox}$; $Mst2^{flox/flox}$ for all figures.

Immunofluorecence. Embryos and hearts were fixed in 4% paraformaldehyde at 4°C for 1 hour, dehydrated in an ethanol series, and paraffin embedded. Sectioned tissues (7μm thick) were deparaffinized in xylene, rehydrated, then microwave-heated for 90 seconds in 10 mM sodium citrate (pH 6.0) for antigen retrieval. Sections were blocked in 2% sheep serum (Sigma, St. Louis, MO) for 30 minutes and incubated in primary antibody at 4°C overnight. Following PBST washes, sections were incubated in broad spectrum biotinylated secondary antibody (PerkinElmer, Shelton, CT) for 10 minutes, followed by incubation with streptavidin-HRP conjugate (PerkinElmer, Shelton, CT) for 10 minutes. Sections were then incubated in fluorescein-labeled tyramid fluorescence signal amplification reagent (PerkinElmer, Shelton, CT) for 10 minutes, followed by counterstaining with TO-PRO®-3 iodide (Molecular Probes, Eugene, OR), then mounted in Aqua-Poly/Mount (Polysciences, Inc., Warrington, PA). Primary antibodies used were as follows: anti-phospho-YAP (1:100), anti-β-catenin (1:100), and anti-phospho Histone H3 Ser-10 (1:100) (Cell Signaling, Danvers, MA); MF20 anti-sarcomeric myosin (1:200) (Developmental Studies Hybridoma Bank, Iowa City, IA); anti-Ddr2 (1:150) (SBT, Santa Cruz, CA); monoclonal anti-Actin/ α-Smooth Muscle -Cy3 (1:200) (Sigma, St. Louis, MO). Immunofluorescent images were captured on a Zeiss 510 confocal microscope, and all functions were controlled via Ziess LSM Image Browser software (Carl Zeiss Microimaging, Inc., Thornwood, NY). All manuscript figures were prepared using Adobe Photoshop CS5 (Adobe Systems Inc., San Jose, CA).

***In situ* hybridization.** Whole-mount *in situ* hybridization was performed using procedures as described previously (*S2*). Details regarding *Sox2* and *Snai2* antisense probes will be provided upon request. At least three wild-type and *Salv CKO* E12.5 embryos were probed in each experiment. Following development of color reactions, hearts were dissected, embedded in OCT medium and sectioned using a Leica CM1850 cryostat (Leica Microsystems, Wetzlar, Germany). Mounted sections were imaged as described in Immunofluorescence.

Histology/Morphometric Analyses. Whole embryos and hearts were fixed and paraffin embedded as described above. Deparaffinized sections (7 μm thick) were rehydrated in a graded ethanol series and stained with hematoxylin and eosin using standard procedures. Images were captured on a Nikon Eclipse 80i upright microscope equipped with a DS-Fi1 digital camera. All measurements and functions were controlled by the NIS-Elements BR3.1 software program (Nikon, Instruments Inc., Mellville, NY). Measurements of myocardium layer thickness and ventricle chamber surface area were obtained from multiple serial sections and averages were obtained. Cell surface area measurements were obtained from LSM images imported into ImageJ software (http://rsbweb.nih.gov/ij/). For all experiments, three control and three Salvador mutant hearts were measured.

Microarray and Quantitative PCR Studies. Dissected E9.5 hearts were placed in RNAlater for tissue stabilization. Total RNA was then extracted using the RNeasy Micro Kit (Qiagen), and concentration was calculated using a SmartSpec Plus™ spectrophotometer (Bio-Rad, Hercules, CA). First strand cDNA synthesis was then performed using SuperScript™ II Reverse Transcriptase kit (Invitrogen, Carlsbad, CA) using 1 μg of total RNA input. DNA microarray analysis was performed using the OneArray™ Mouse Whole Genome Array that interrogated 17,455 unique genes using 29,972 probes (Phalanx Biotech Group, Palo Alto, CA). For real-time quantitative PCR, 2 μl of cDNA (1:10 dilution) was added to Brilliant II SYBR Green QPCR Master Mix (Stratagene, Santa Clara, CA) in triplicate reactions and run on a Mx3000P QPCR System (Stratagene, Santa Clara, CA). Sequences of primers used in qPCR are listed in Table S2.

Cell counting/β-catenin tabulation. To quantify the index of specific cell-types within ventricle tissues, serial sections of E12.5 hearts immunostained with antibodies specific to cardiomyocytes (α-MF20), smooth muscle (α-smooth muscle actin), or fibroblasts (α-Ddr2) were imaged at 40x magnification and cells were counted manually. Within each field of view, nuclei were counted using ImageJ software. To obtain a sampling of individual hearts, no less than 15 evenly spaced sections were analyzed per specimen (control (n=3), *Salv CKO* (n=3)). To assess the percentage of ventricular cells with nuclear β-catenin localization, cells were counted manually selecting for cells that exhibit a discrete anti-β-catenin/TO-PRO-3 overlap. To determine ventricular cardiomyocyte proliferation indices, cells displaying an MF20/pHH3 overlap were counted manually. pHH3-positive nuclei were counted manually in all proliferation studies. Nuclei counts and sampling for all experiments were performed as described above.

ChIP analysis. Cells were treated with 1% formaldehyde for 15 min to cross-link histones to DNA. Cells were then washed twice in cold PBS, washed for 5 min in cross-link buffer (0.125 M Glycine, 1 mM EDTA, 0.5 mM EGTA, 50 mM HEPES, pH 7.9) followed by two PBS washes. Cells were resuspended in 300 ml lysis buffer (50 mM Tris-HCl, pH 8.1, 10 mM EDTA, 1.0% SDS) supplemented with protease inhibitors and sonicated for 1 min at 10 sec intervals. Purified DNA fragments were analyzed on 1.5-2.0% agarose gels to determine chromatin shearing efficiency. Lysates were diluted 10-fold in dilution buffer (20 mM Tris-HCl, pH 8.1, 150 mM NaCl, 2 mM EDTA, 1.0% Triton X-100), pre-cleared with 55 ml Protein A/G Plus agarose slurry (SBT, Santa Cruz, CA) for 2 hours at 4°C, then rocked overnight at 4°C with appropriate primary antibodies: anti-YAP (1:50) (Cell Signaling, Danvers, MA); anti-β-catenin (1:50) (SBT, Santa Cruz, CA); monoclonal anti-β-catenin (Biotinylated) (1:50) (Cell Signaling, Danvers, MA). 55 ml Protein A/G Plus agarose was added to each sample for 1 hr incubation at 4°C. Immunoprecipitates were washed once with TSE I buffer (150 mM NaCl, 20 mM Tris-HCl, pH

8.1, 0.1% SDS, 1.0% Triton X-100), once in TSE II buffer (500 mM NaCl, 20 mM Tris-HCl, pH 8.1, 0.1% SDS, 2 mM EDTA, 1.0% Triton X-100), once in LiCl buffer (250 mM LiCl, 10 mM Tris-HCl, pH 8.1, 1 mM EDTA, 1.0% NP-40 (EGEPAL), 1.0% Triton X-100) and twice in TE buffer (10 mM Tris-HCl, pH 8.1, 1 mM EDTA). Immunoprecipitates were eluted in 250ml elution buffer (100 mM $NaHCO_3$, 1.0% SDS) at room temperature for 15 min. Cross-links were reversed by heating samples at 65°C for 4 hr, and samples were then treated with proteinase K for 1hr at 45°C. DNA was extracted with phenol/chloroform and was ethanol-precipitated. The following primer pairs were used for the amplification of PCR product: *Sox2* 5′-CCTGCCATGTCGCCAGTTCCT-3' and 5′-CCTCGCGCACACAAAGGC ACG -3′; *Snai2* 5′-GCAGTAAATGTGCAAGCTC-3' and 5′- CCTACTTAGGAATGATCCAAAG-3'. As a control, normal rabbit immunoglobulin G was used as a replacement for Yap or β-catenin antibodies. In addition to the above listed steps, procedures as described previously (*S3*) were incorporated for sequential ChIP

Luciferase Assays. To generate *Sox2* and *Sox2* (-Tead site) enhancer element reporter plasmids, 1011 and 747bp of genomic sequence were amplified respectively using Phusion High fidelity Polymerase (New England Biolabs, Ipswich, MA) with the following primers: *Sox2*: (sense) CGGGATCCGCGACACATTCTTGCAGTGGG (underlined: BamHI subcloning site), (antisense) ACGCGTCGACGTGCTTCCAATCCCAAGATAGG-3' (underlined: SalI subcloning site); *Sox2* (-Tead): (sense) CGGGATCCGGTAGTAATTACAGCCCAATTC (underlined: BamHI subcloning site), (antisense) ACGCGTCGACCTCCTAGATAGAGTCCCTAGG (underlined: SalI subcloning site). To generate *Snai2* and *Snai2* (-Tead site) enhancer element reporter plasmids, 1043 and 953bp of genomic sequence amplified as per *Sox2* with the following primers: *Snai2*: (sense) CGGGATCCGAAGGCCACTGCTCCTCCCTCCC (underlined: BamHI subcloning site), (antisense) ACGCGTCGACCCTCTTGACATCTGTATGCCT (underlined: SalI subcloning site); *Snai2* (-Tead): (sense) CGGGATCCGAAATAGTTTTGAGGTTCTTTGG (underlined: BamHI subcloning site), (antisense) ACGCGTCGACCCAACCCTTCTATATATG (underlined: SalI subcloning site). Digested fragments were subcloned into the pGL3-Promoter Vector (Promega, Madison, WI) and sequenced accordingly. The luciferase assays were performed as described previously (*S4*).

Coimmunoprecipitation and Immunoblotting. E14.5 hearts were treated with RIPA lysis buffer (50 mM Tris-HCl (pH 7.4), 150 mM NaCl, 1 mM EDTA, 0.5% sodium deoxycholate, 0.1% SDS, 1% Triton X-100) supplemented with protease and phosphatase inhibitors (Sigma, St Louis, MO) and sonicated over ice. Supernatants of centrifuged lysates were collected and protein concentration was determined using Pierce® BCA Protein Assay Kit (Pierce Biotechnology, Rockford, IL). Lysates were pre-cleared and incubated with appropriate antibodies [anti-YAP (1:50) (Cell Signaling, Danvers, MA); anti-β-catenin (1:50) (SBT, Santa Cruz, CA)] as described above. Protein A/G Plus agarose was added to each sample for 1 hr incubation at 4°C and samples were washed three times in TBST (TBS + 0.1% Triton X-100). Immunoprecipitates were eluted by boiling for three minutes in 20 ml of 2x sample buffer (125 mM Tris-HCl, pH 6.8, 4% SDS, 20% (v/v) glycerol, 0.004% bromophenol blue). Following separation via SDS PAGE, proteins were transferred to PDVF membranes, blocked in 2% milk/TBST and incubated with appropriate primary antibodies overnight at 4°C. Membranes were then washed three times in TBST and incubated with HRP-conjugated secondary antibodies

(1:3000) (Bio-Rad, Hercules, CA) for two hours at room temperature. Following TBST washes, protein detection was performed using SuperSignal West Pico Chemiluminescent Substrate (Thermo Scientific, Rockford, IL). For quantitation, pYAP, total Yap and α-tubulin Western Blot band densities for control (*Nkx2.5*$^{Cre/+}$; *Salv*$^{flox/+}$) and *Salv CKO* were determined using ImageJ software. To determine relative pYAP and total YAP levels, data was normalized against α-tubulin as a protein loading control.

Statistical Analysis. For all experiments conducted in this study, data are presented as mean values ± standard error (SEM). p-values were calculated using unpaired Students t-tests comparing control and mutant hearts. Statistically significant differences ($p<0.01$) are indicated by asterisks.

SUPPLEMENTAL FIGURES

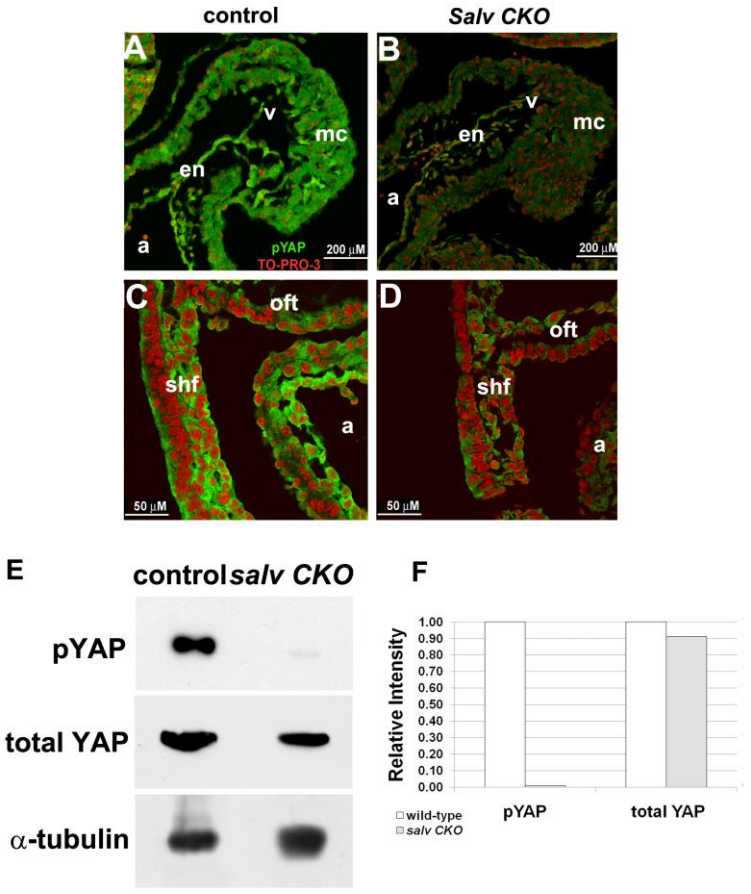

Figure S1: Salvador deletion reduces cardiac Hippo activity. (A-D) control (A, C) and *salv CKO* (B, D) E9.5 sagittal heart sections: TO-PRO-3 (red) and pYAP antibodies (green). a (atrium), en (endocardium), v (ventricle), mc (myocardium), shf (second heart field), oft (outflow tract). (E) Western: E14.5 heart extracts with designated antibodies. (F) pYAP and total Yap levels for control (*Nkx2.5*$^{Cre/+}$; *Salv*$^{flox/+}$) and *Salv CKO* in E were determined and normalized against α-tubulin as a protein loading control.

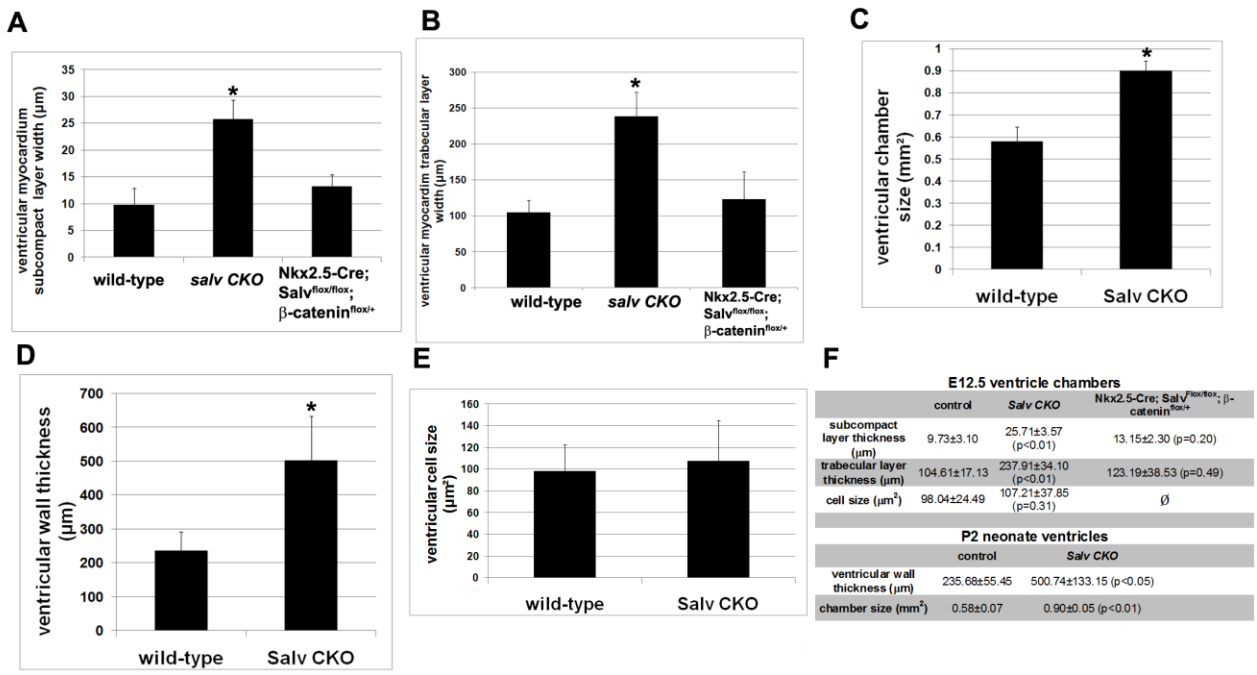

Figure S2: Morphometric measurement of Salvador mutant heart size. (A-B) Measurement of ventricular subcompact (A) and trabecular (B) myocardium layer thickness was performed in E12.5 coronal heart sections. (C-D) Surface area measurement of ventricle chamber size (C) and ventricular wall thickness (D) was performed in P2 neonate heart sections. (E) Surface area measurement of ventricle cell size was performed in E12.5 coronal heart sections. p = 0.31. (F) Tabulation of A-E.

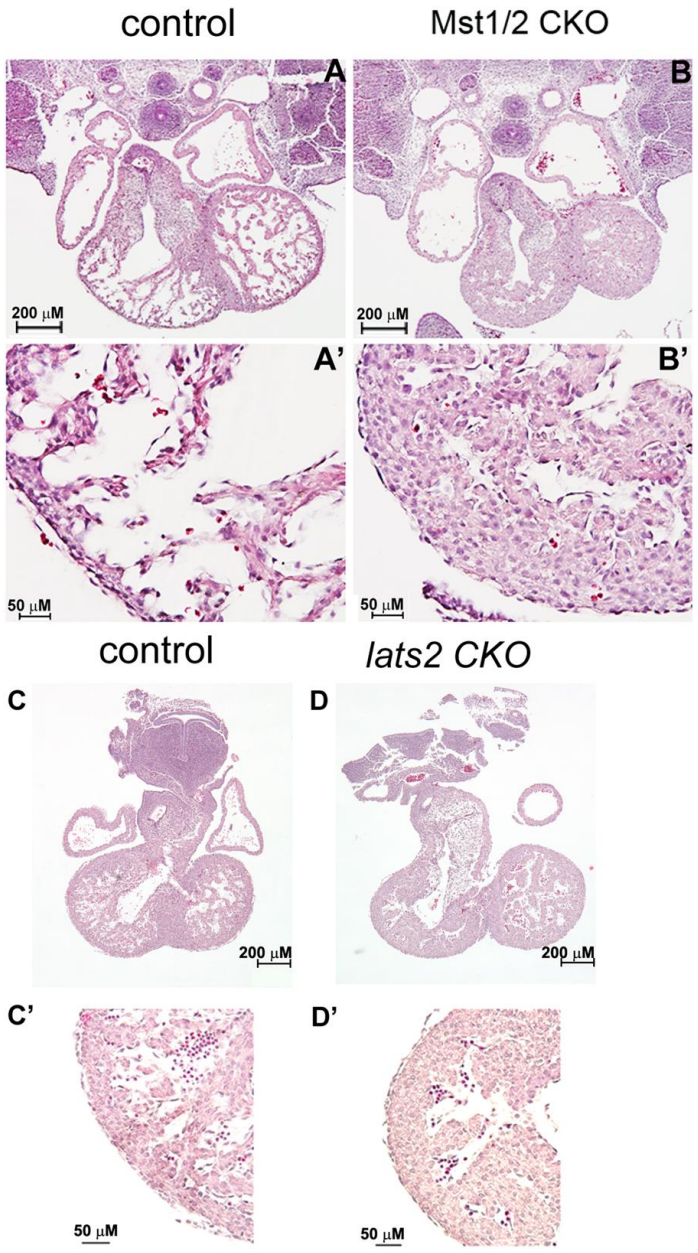

Figure S3: Cardiac phenotype of *mst1-2* and *lats2* mutants. (A-B) Images of E11.5 control (A, A') and *mst1-2 CKO* (B, B') H&E-stained coronal heart sections. A' and B' are high magnification images of the myocardium from A and B respectively. Control: *Nkx2.5*$^{Cre/+}$; *mst1*$^{flox/+}$; *mst2*$^{flox/+}$. (C-D) Images of E11.5 control (C, C') and *lats2 CKO* (D, D') H&E-stained coronal heart sections. C' and D' are high magnification images of the myocardium from C and D respectively. Control: *Nkx2.5*$^{Cre/+}$; *lats2*$^{flox/+}$.

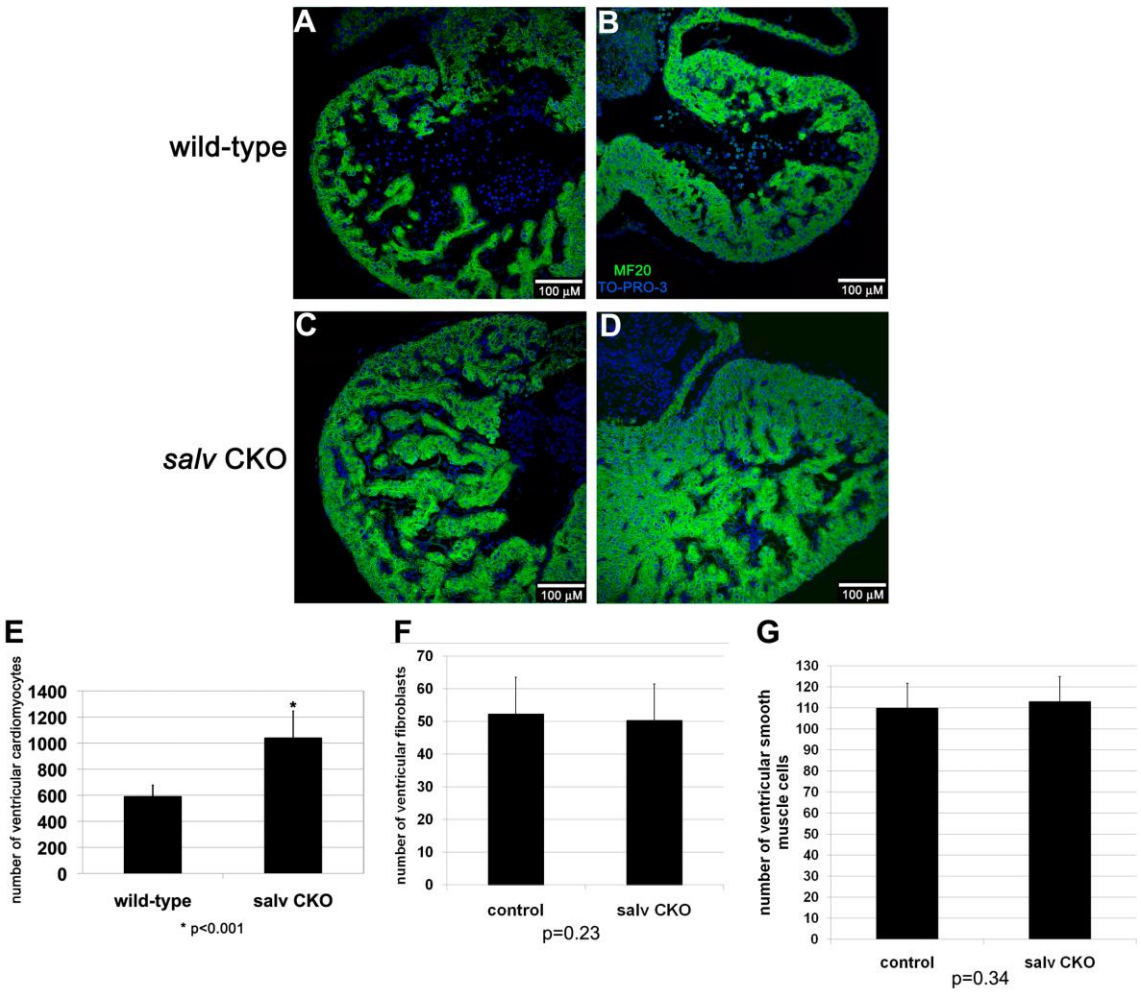

Figure S4: Increased number of cardiomyocytes in Salvador mutant ventricles. (A-E) E12.5 control (A, B) and *salv CKO* (C, D) coronal heart sections were fixed and stained with TO-PRO-3 (blue) and cardiomyocyte-specific antibodies (α-MF20, green). Representative images of wild-type (A, B) and *salv CKO* (C, D) right and left ventricles are shown. (E) Quantification of cardiomyocytes within ventricles. MF20-positive cells were counted manually while nuclei were counted as described in Figure 2C. (F, G) Quantification of fibroblast and smooth muscle cell number within ventricles. Control and *salv CKO* E12.5 heart sections were treated with α-DDR2 (F) and α-smooth muscle actin (α-SMA; G) antibodies, markers for fibroblast and smooth muscle respectively. Indices of these cell types within ventricles were determined as described earlier.

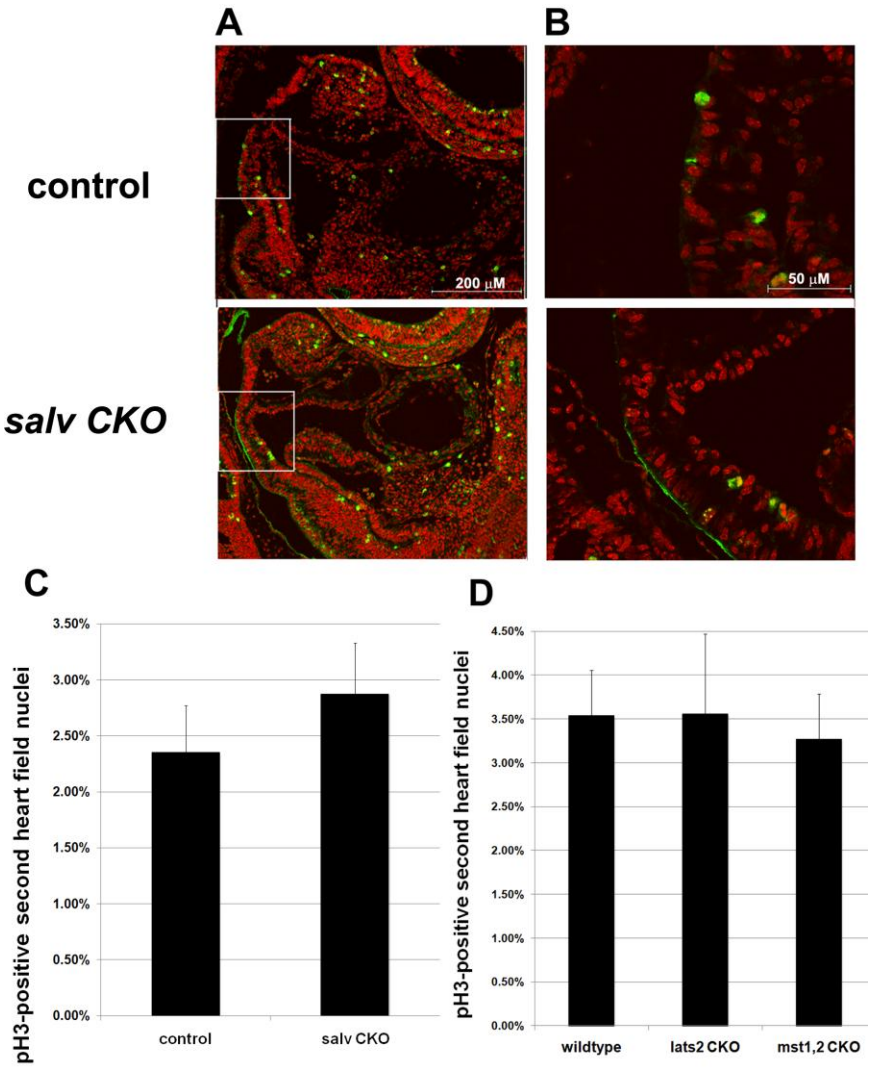

Figure S5: Hippo signaling does not regulate proliferation of cardiac progenitors. (A-B) E9.5 sagittal control (A) and *salv CKO* (B) heart sections were fixed and stained with pHH3 antibodies (green) and nuclei were counterstained with TO-PRO-3 (red). Images in the right lane (B) are high magnification views of second heart field tissue as boxed in A. (C-D) Quantification of pHH3-positive second heart field nuclei within control, *salv CKO*, *lats2 CKO*, and *mst1-2 CKO* E9.5 hearts.

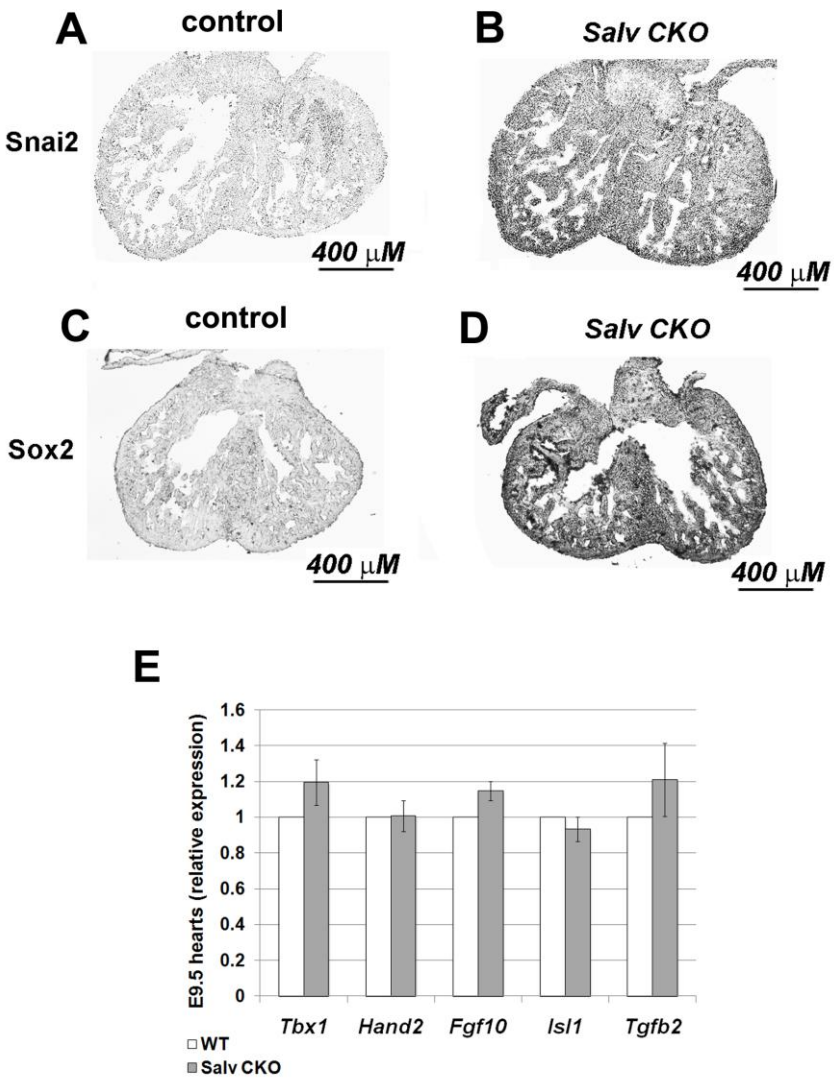

Figure S6: Gene expression changes in Salvador mutant hearts. (A-D) Whole mount *in situ* hybridization of E12.5 control (A, C) and *salv CKO* (B, D) hearts. Frozen sections of hearts treated with digoxigenin (DIG) labeled *Snai2* (A-B) and *Sox2* (C-D) antisense mRNA probes are displayed. (E) qPCR reveals similar expression of second heard field genes in *Salv CKO* hearts. Values were determined as in Figure 3B.

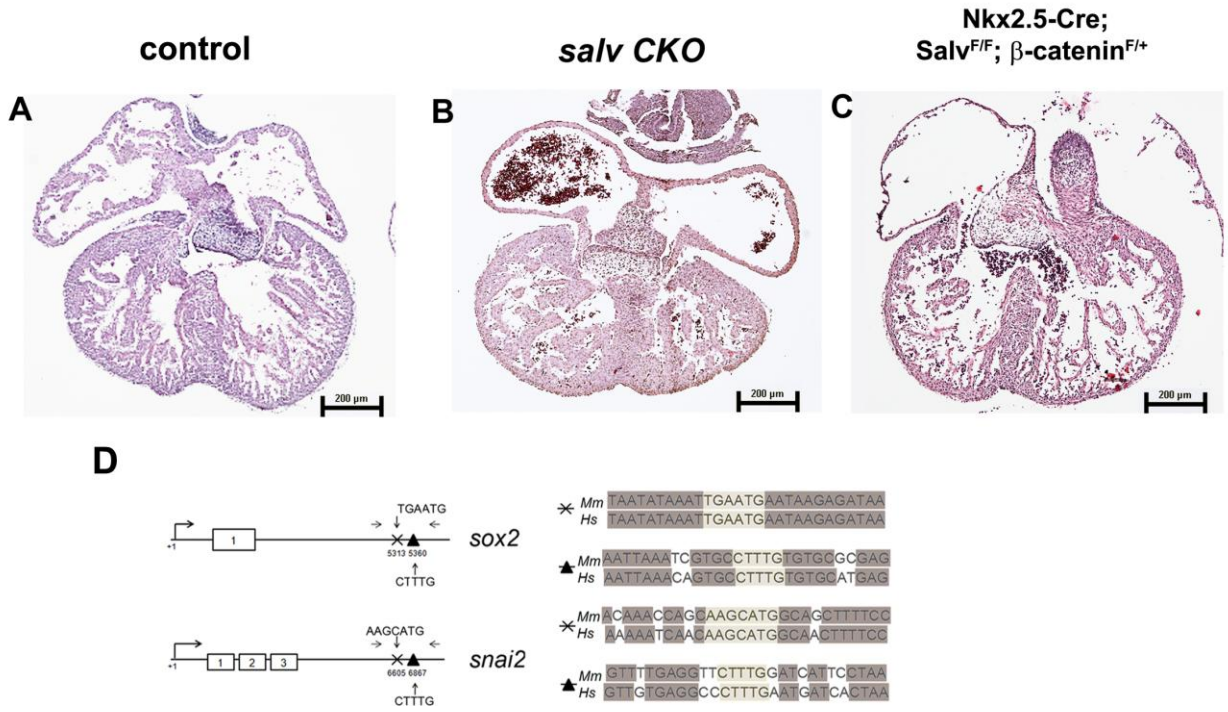

Figure S7: Wnt/Hippo regulation of cardiac growth. (A-C) H&E staining of control (A), *salv CKO* (B), and *Nkx2.5^{Cre}; Salv$^{F/F}$; β-catenin$^{F/+}$* (C) E12.5 hearts. (D) Diagram of *Sox2* and *Snai2* downstream sequences assayed via chromatin immunoprecipitation (ChIP). X and Δ: sites assayed for YAP and β-catenin ChIP. Light gray highlighted sequences are conserved YAP/TEAD and Lef/TCF binding elements respectively. Arrows: locations of primer sequence used in ChIP PCR. Boxes 1, 2, and 3 (exons of *Sox2* and *Snai2* ORFs). *Hs* (*Homo sapiens*) and *Mm* (*Mus musculus*).

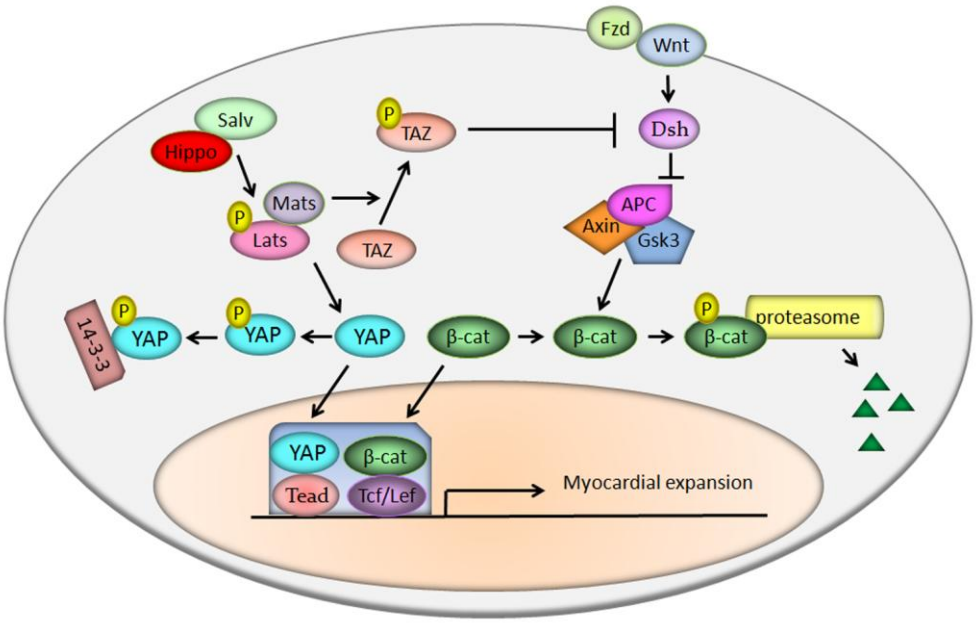

Figure S8: Model for Wnt/Hippo regulation of cardiac growth. When cardiac Hippo activity is high, phosphorylation of downstream effector molecules YAP and TAZ is upregulated. Nuclear entry of phosphorylated of YAP is thereby prevented whereas phosphorylated TAZ represses Dishevelled (Dsh) inhibition of the β-catenin destruction complex. When the Hippo pathway is silenced, Dsh inhibition by TAZ is downregulated whereas Yap can freely localize to the nucleus and complex with Tead/Tef factors and β-catenin to promote expression of cardiac growth factors.

SUPPLEMENTARY TABLES

F1 genotype frequencies from Nkx2.5-Cre/+; $Salv^{flox/+}$ x $Salv^{flox/flox}$ matings

Genotype	E9.5		E10.5		E11.5	
	Expected	Observed	Expected	Observed	Expected	Observed
$Nkx2.5^{+/+}$; $Salv^{flox/+}$	~23.5/94 (25%)	23/94 (24.5%)	~11.75/47 (25%)	9/47 (19.1%)	~9.5/38 (25%)	7/38 (~18.5%)
$Nkx2.5^{+/+}$; $Salv^{flox/flox}$	~23.5/94 (25%)	20/94 (~21.2%)	~11.75/47 (25%)	14/47 (29.8%)	~9.5/38 (25%)	11/38 (28.9%)
Nkx2.5-Cre/+; $Salv^{flox/+}$	~23.5/94 (25%)	23/94 (24.5%)	~11.75/47 (25%)	11/47 (23.4%)	~9.5/38 (25%)	9/38 (23.7%)

Genotype	E12.5		E14.5		E16.5	
	Expected	Observed	Expected	Observed	Expected	Observed
$Nkx2.5^{+/+}$; $Salv^{flox/+}$	28/112 (25%)	30/112 (~26.8%)	~20.5 (25%)	24/82 (29.3%)	~7.25/29 (25%)	9/29 (31.0%)
$Nkx2.5^{+/+}$; $Salv^{flox/flox}$	28/112 (25%)	27/112 (~24.1%)	~20.5 (25%)	23/82 (28.0%)	~7.25/29 (25%)	6/29 (20.7%)
Nkx2.5-Cre/+; $Salv^{flox/+}$	28/112 (25%)	29/112 (~25.9%)	~20.5 (25%)	17/82 (20.7%)	~7.25/29 (25%)	8/29 (27.6%)
Nkx2.5-Cre/+; $Salv^{flox/flox}$	28/112 (25%)	26/112 (~23.2%)	~20.5 (25%)	18/82 (22.0%)	~7.25/29 (25%)	6/29 (20.7%)

Genotype	P2*	
	Expected	Observed
$Nkx2.5^{+/+}$; $Salv^{flox/+}$	~20/79 (25%)	22/79 (~27.9%)
$Nkx2.5^{+/+}$; $Salv^{flox/flox}$	~20/79 (25%)	23/79 (29.1%)
Nkx2.5-Cre/+; $Salv^{flox/+}$	~20/79 (25%)	26/79 (32.9%)
Nkx2.5-Cre/+; $Salv^{flox/flox}$	~20/79 (25%)	8/79 (10.1%)

*χ^2 = 9.759 (df=3; p=0.0207)

Table S1: Perinatal lethality of Salvador mutant mice. Genotype tabulation of litters at indicated stages. Chi-square analyses based on predicted Mendelian ratios were performed for each stage. Approximately 40% of the expected number Salvador mutant progeny arise at the P2 neonatal stage.

Gene	Forward	Reverse
Birc2	AAGGTGTGAGTTCTTGATACGG	CTCCTACTGAAGCCCATTTCC
Birc5	GCTGTACCTCAAGAACTACCG	CTTGACAGTGAGGAAGGCG
Bmp4	AGGAAGAGCAGAGCCAGGGAA	TGCTGCTGAGGTTGAAGAGGAAAC
Cdc20	GGCACATTCGCATTTGGAACG	TAGTGGGGAGACCAGAGGATGGAG
Fgf10	AGTGTCCTGGAGATAACATCAGTGG	TTTGCCTGCCATTGTGCTGC
Hand2	CTTCAAGGGCCCAAGATTC	CTCAGCGCATCCATTTTCTA
Isl1	CTTTTCTGCCGTGCAGACCACGAT	CAGCTGCTTCTCGTTGAGCACAGT
Mycl1	ACGGCACTCCTAGTCTGG	GGTGGATAGAGATATGGAAGTGC
Snai2	TGTGTCTGCAAGATCTGTGG	TGGAGAAGGTTTTGGAGCAG
Sox2	ATGCACAACTCGGAGATCAG	TGAGCGTCTTGGTTTTCCG
Tbx1	CGACAAGCTGAACTGACCA	CAATCTTCCGCTGCGTGATCC
Tgfb2	TGGAGTTCAGACACTCAACACA	AAGCTTCGGGATTTATGGTGT

Table S2: List of Primer Sequences used in reverse quantitative PCR (qPCR)**.**

SUPPLEMENTAL REFERENCES

S1. K. A. Moses, F. DeMayo, R. M. Braun, J. L.Reecy, R. J. Schwartz. *Genesis* **4**, 176 (Dec, 2001).

S2. D. Ai, X. Fu, J. Wang, M. F. Lu, L. Chen, A. Baldini, W. H. Klein, J. F. Martin. *PNAS* **104**, 9319 (May, 2007).

S3. R. B. Medeiros, K. J. Papenfuss, B. Hoium, K. Coley, L. Jadrich, S. K. Goh, A. Elayaperumal, J. E. Herrera, E. Resnik, H. T. Ni. *BMC Biotechnol* **9**, 59 (June, 2009).

S4. J. Wang, S. B. Greene, M. Bonilla-Claudio, Y. Tao, J. Zhang, Y. Bai, Z. Huang, B. L. Black, F. Wang, J. F. Martin. *Dev Cell* **19**, 903 (Dec, 2010).